

Computer-Aided Design of Tailor-Made Ionic Liquids

Arunprakash T. Karunanithi and Amirhossein Mehrkesh

Dept. of Civil Engineering, University of Colorado Denver, 1200 Larimer Street, Denver, CO 80217

DOI 10.1002/aic.14228

Published online October 21, 2013 in Wiley Online Library (wileyonlinelibrary.com)

Ionic liquids (IL), with their negligible vapor pressure, have the potential to replace volatile organic solvents in several processes. They also exhibit other unique characteristics, such as high thermal stability, wide liquid range, and wide electrochemical window, which make them attractive for many important applications. In addition, millions of ILs can be formed through different combination of cations, anions, and other functional groups. Till now, majority of work on IL selection, for a given application, is guided by trial and error experimentation. In this article, we present a computer-aided IL design framework, based on semiempirical structure-property models and optimization methods, which can consider several IL candidates and design optimal structures for a given application. This powerful methodology has great potential to act as a knowledge-based framework to aid synthetic chemists and engineers develop new ILs. © 2013 American Institute of Chemical Engineers AIChE J, 59: 4627–4640, 2013

Keywords: ionic liquids, computer-aided molecular design, optimization, physical properties

Introduction

Ionic liquids (ILs) are an alternative class of solvents that are increasingly being applied in chemical synthesis and other applications.¹ They are entirely composed of ions and the first IL—triethylammonium nitrate—was discovered more than a century ago.² ILs are essentially salts that have low melting temperature and consist of a large organic cation and a charge-delocalized inorganic or organic anion of smaller size and asymmetric shape.³ They have excellent solvation properties for a variety of inorganic, organic, and polymeric materials. They possess good thermal stability and do not decompose over a large temperature range making them useful for carrying out reactions that require high temperatures.¹ ILs also offer a wide liquid temperature range making them attractive as liquid solvents. ILs are nonvolatile and are rarely flammable or explosive, thereby presenting fewer environmental risks and health hazards. These characteristics have led to the emergence of ILs as alternative solvents for several applications.

There exists a large library of anions and cations.^{4,5} Similar to organic compounds, where the atoms carbon, hydrogen, and oxygen can be combined to form thousands of alternative molecular structures ILs can be formed through any combination of cations, anions, and alkyl groups attached to the cation head group leading to several structural possibilities (estimated to be as many as 10^{14} combinations).^{6,7} This is due to the fact that ILs are composed of organic cations and these organic compounds can have unlimited structural variations due to the easy

nature of preparation of many components.⁸ Moreover, synthesis of a wide range of ILs is relatively straightforward. This presents a great opportunity to engineer ILs that have specific properties. Task specific ILs can be designed for a particular application by controlling the physicochemical properties by judicious selection/modification of the cation, the anion, and/or the alkyl chains attached to the cation. This also presents an unusual challenge, where synthesizing, screening, and testing the limitless possibilities becomes an impossible task.⁹

This is where *in silico* methods could act as a valuable tool for discovering new ILs with tailored properties. Up until now, majority of IL computational studies are based on *ab initio* methods such as molecular dynamics, and quantum chemical calculations.^{10–13} These methods are extremely important and offer useful insights as they are able to predict properties without performing costly experiments. However, as in the case of experiments, one needs to perform several individual simulations which again is impractical due to the long simulation times required for statistical averaging. Both molecular dynamic simulations and experiments are necessary and important steps in the selection of task specific ILs. Nevertheless, these are steps to be applied at the final stages of IL selection. The missing piece is a method for fast exploration, design, and identification of a subset of promising candidates, from the millions of IL alternatives that are available.

Computer-aided molecular design (CAMD) is a promising approach that has been widely applied for molecular systems to design organic solvents for a variety of applications.^{14–20} It integrates property prediction models and optimization algorithms to reverse engineer molecular structures with unique properties. We believe that a similar approach is even more relevant for the design of ILs due to the numerous ionic combinations that are possible.

Correspondence concerning this article should be addressed to A. Karunanithi at arunprakash.karunanithi@ucdenver.edu.

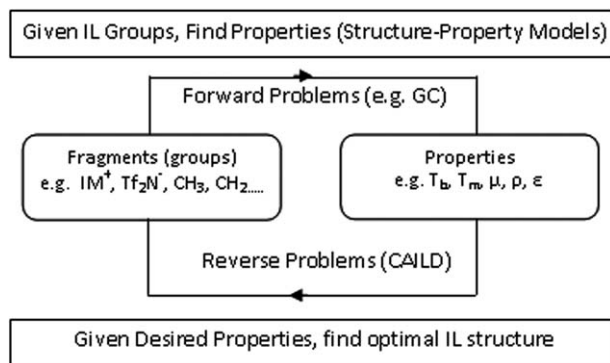


Figure 1. CAILD framework.

Computer-Aided Ionic Liquid Design (CAILD)

In this article, we present an overarching framework that aims to identify ILs that exhibit certain desirable behavior. Here, the identity of the compound (in this case IL) is not known *a priori*, but we can specify the properties that the compound (i.e., IL) needs to have.¹⁴ This approach termed as CAILD can be defined as “given a set of IL functional groups (i.e., base cations: Im^+ , Py^+ , NH_4^+ ; anions: Cl^- , Tf_2N^- , BF_4^-; side chain groups: CH_3 , $=\text{O}$, $-\text{S}-$, OH) and a specified set of target properties (e.g., melting point, electrical conductivity, viscosity, solubility....) find an IL structure that matches these properties.”

Intuitively, CAILD can be thought of as a reverse problem of structure (or group) based property prediction as shown in Figure 1. In the forward problem (property prediction), we know the IL structure and are interested in its properties. In the reverse problem (CAILD), we know the target property values (or ranges) and are interested in feasible IL structures. To implement CAILD, we need: (1) a framework to fragment ILs into groups; (2) combination and feasibility rules to identify chemically feasible ILs; (3) structure (or group)-based models for property prediction; and (4) optimization framework to search through millions of available alternatives. Mathematical programming approach provides a useful mechanism to solve such CAILD problems. Several approaches including generate and test approach (e.g., Harper et al.),²¹ and optimization approaches (e.g., Sahinidis and coworkers)²² have been used to solve such problems. The solution to the underlying mixed integer nonlinear programming (MINLP) model will result in the optimal molecu-

lar structure for the given application. The objective function is usually an important property related to the design problem, whereas the constraints relate to structural feasibility, pure component properties, solution (mixture) properties, and equilibrium relationships. A conceptual representation of this approach is shown in Figure 2.

In this study for computer-aided design of ILs, a comprehensive approach in five sections is proposed. First section will focus on describing the general mathematical framework of the proposed approach; second section deals with structural constraints, providing an in-depth mathematical treatment of feasibility, complexity, and bonding rules required to design chemically feasible ILs; third section deals with physical property constraints where group contribution (GC)-based structure-property models are discussed for predicting IL physical (pure component) properties; fourth section focuses on solution property constraints that utilize the functional group concept-based models, such as UNIFAC, for calculation of solution (mixture) properties through activity coefficients; fifth section focuses on operations research methods for solving the proposed optimization model.

Mathematical framework

The generic mathematical formulation of the CAILD model as an optimization problem is shown in Eqs. 1–11. This formulation takes the form of MINLP model.

$$f_{\text{obj}} = \max f(c, a, y, ng, x) \quad (1)$$

$$h_1(c, a, y, ng) = 0 \quad (2)$$

$$h_2(c, a, y, ng) \leq 0 \quad (3)$$

$$g_2(c, a, y, ng) \leq 0 \quad (4)$$

$$d_1(c, a, y, ng, x) = 0 \quad (5)$$

$$d_2(c, a, y, ng, x) \leq 0 \quad (6)$$

$$c \in \mathbb{R}^m \quad (7)$$

$$a \in \mathbb{R}^n \quad (8)$$

$$y \in \mathbb{R}^u \quad (9)$$

$$ng \in \mathbb{R}^q \quad (10)$$

$$x \in \mathbb{R}^r \quad (11)$$

where h_1 is a set of structural feasibility and complexity equality constraints, h_2 is a set of structural feasibility and complexity inequality constraints, g_2 is a set of pure component physical property inequality constraints, d_1 is a set of equality design constraints, d_2 is a set of solution (mixture)

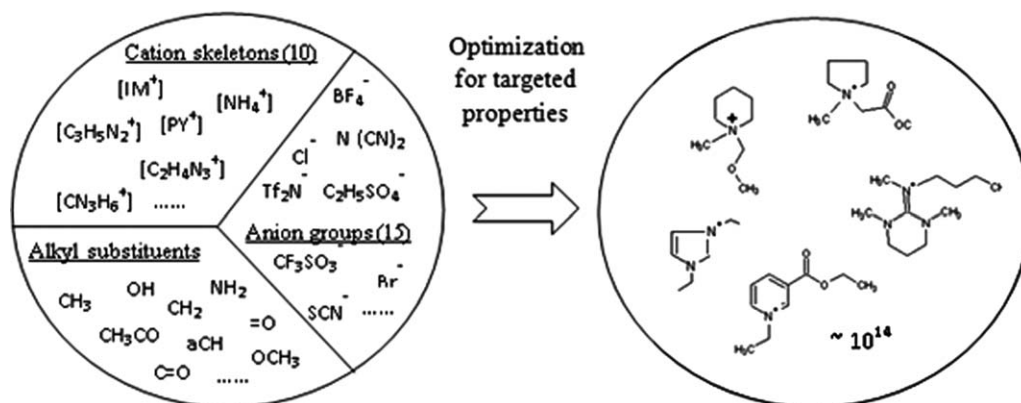


Figure 2. Conceptual description of CAILD.

property inequality design constraints, c is a m -dimensional vector of binary variables denoting cation base groups, a is a n -dimensional vector of binary variables denoting anion, y is a u -dimensional vector of binary variables denoting the alkyl side chains, ng is a q -dimensional vector of integer variables representing number of groups in the alkyl side chains, and x is a r -dimensional vector of continuous variables representing compositions, flow rates, and so forth.

IL structural constraints

The designed ILs need to satisfy certain rules to ensure chemical feasibility. These rules, termed as structural constraints, include feasibility rules such as octet rule, bonding rule, and complexity rules. Similar rules have been previously developed for molecular compounds.^{23,24} Equations 12–24 represent a comprehensive set of constraints that were developed to ensure design of IL candidates that are chemically feasible.

$$\sum_{i \in c} c_i = 1 \quad (12)$$

$$\sum_{j \in a} a_j = 1 \quad (13)$$

$$\sum_{l=1}^6 y_l = \sum_{i \in c} c_i v_{ci} \quad (14)$$

$$\sum_{i \in c} (2 - v_{ci}) c_i + \sum_{l=1}^6 \sum_{k \in G} (2 - v_{Gkl}) y_l n_{Gkl} = 2 \quad (15)$$

$$\sum_{k \in G} y_l n_{Gkl} (2 - v_{Gkl}) = 1 \quad (16)$$

$$\sum_{l=1}^6 \sum_{k \in G} y_l n_{Gkl} \leq n_G^U \quad (17)$$

$$\sum_{k \in G} y_l n_{Gkl} \leq n_{Gl}^U \quad (18)$$

$$\sum_{k \in G^*} y_l n_{Gkl} \leq t_1 \quad (19)$$

$$\sum_{k \in G^*} y_l n_{Gkl} \geq t_2 \quad (20)$$

$$\sum_{k \in G^*} y_l n_{Gkl} = t_3 \quad (21)$$

$$\sum_{l=1}^6 \sum_{k \in G^{**}} y_l n_{Gkl} \leq t_4 \quad (22)$$

$$\sum_{l=1}^6 \sum_{k \in G^{**}} y_l n_{Gkl} \geq t_5 \quad (23)$$

$$\sum_{l=1}^6 \sum_{k \in G^{**}} y_l n_{Gkl} = t_6 \quad (24)$$

where c_i is a vector of binary variables representing the cations and a_i is a vector of binary variables representing the anions. y_l is a vector of binary variables representing the alkyl chains. ng_{kl} is a vector of integer variables representing the number of groups of type k in the alkyl side chain l . v_{ci} , v_{Gkl} are vectors of group valencies of the cations and alkyl groups, respectively. G is the set of all alkyl groups available for the cation side chains. Eqs. 12 and 13 ensures a maximum of one cation base and one anion, respectively, for each IL candidate. Eq. 14 fixes the number of alkyl side

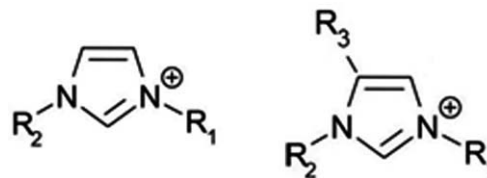


Figure 3. A general Scheme of two feasible cation structures.

chains attached to the cation based on available free valence of the cation base. *Modified octet rule*: The implementation of the modified octet rule (Eq. 15) ensures that any designed cation is structurally feasible and that each valency in all structural groups of the cation is satisfied with a covalent bond. Note that this formulation has already accounted for the positive charge associated with the cation. Equation 16 ensures that the octet rule is implemented for each side chain l to ensure that the valences in the individual chains are satisfied with a covalent bond. *Cation size*: The size of the cation is controlled by introducing an upper bound on maximum number of groups n_G^U that are allowed in the cation (Eq. 17). *Alkyl chain size*: The size of the alkyl chains are controlled by introducing an upper bound on the maximum number of groups n_{Gl}^U that can be present in each alkyl side chain (Eq. 18). Equations 19–21 can be utilized to place restrictions on number of occurrences (t_1 , t_2 , and t_3) of a certain group, G^* , in each side chain l . In other words, Eq. 19 can be used to make sure that a certain main group such as aldehyde or alcohol not being present more than a certain number of times in each side chain of the cation, and Eq. 20 can be applied when we want a certain group to be present at least t_2 times, and Eq. 21 can be used when an exact number of occurrence of a certain group is desired, for example, when we want to have exactly one aldehyde group in a certain side chain in the cation. Equations 22–24 can be utilized to place restrictions on number of occurrences (t_4 , t_5 and t_6) of a certain group G^{**} , in the cation, which can be calculated as summation of number of occurrences of the particular group in all the side chains in the cation. The purpose of Eqs. 22–24 is exactly similar to that of Eqs. 19–21 with the difference of placing restrictions on the number of occurrences of a particular group in whole cation (summation of all of the side chains) instead of only one side chain.

The cation related structural feasibility constraint (Eq. 14) is explained using the generic cation dialkylimidazolium (shown in Figure 3a) as an example. According to the proposed formulation the valency for this cation is 2 (i.e., $v_{ci}=2$), as there are two alkyl side chains (R_1 and R_2) that are allowed. Similarly, the valency of a trialkylimidazolium (shown in Figure 3b) is 3. For dialkylimidazolium, the right-hand side (RHS) of Constraint 3 (Eq. 14) will translate into $\sum_{i \in c} c_i v_{ci} = (1)(2) = 2$, which will fix the left-hand side (LHS) of Constraint 3 as $\sum_{l=1}^6 y_l = 2$, that is, $[y_1=1]$ and $[y_3=1]$. Therefore, the vector y , will take the following values [101000] with the two ones representing the presence of two alkyl side chains at positions 1 and 3. Next, with the use of few feasible and infeasible examples shown in Figure 4, we explain how the whole set of feasibility constraints (Eqs. 12–16) work. Figure 4a shows a feasible IL, 1,3-diethylimidazolium tetrafluoroborate. The cation valency and alkyl group valences related to this IL are listed in Table 1.

The values related to the vectors y_l and ng_{kl} for this IL are listed in Table 2.

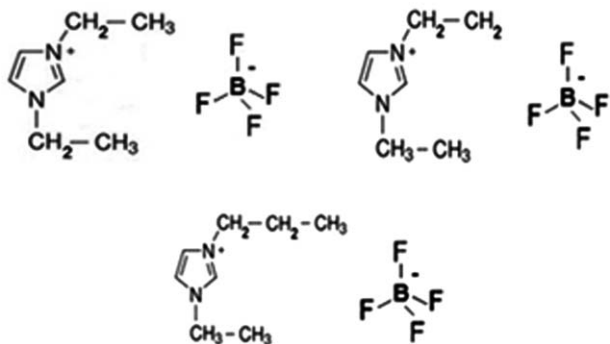


Figure 4. Examples of feasible and nonfeasible ILs.

In this case, there is only one cation base (Eq. 12 is satisfied) and one anion (Eq. 13 is satisfied). The number of side chains are 2 which equates to the valency of cation (Eq. 14 is satisfied). Now, LHS of Eq. 15 translates into $(2 - 2)(1) + [(2 - 2)(1)(1) + (2 - 1)(1)(1)] + [(2 - 2)(1)(1) + (2 - 1)(1)(1)] = 2$ which is equal to RHS of the equation (Eq. 15 is satisfied). For both of the side chain positions (l) 1 and 3, LHS of Eq. 16 translates into $[(1)(1)(2 - 1) + (1)(1)(2 - 2)] = 1$ which is equal to RHS of the equation (Eq. 16 is satisfied). Equations 17 through 24 are only used to control the cation size and place restrictions on the type and number of occurrences of select groups. As such these are not feasibility constraints but user specified structural design constraints. Figure 4b shows an infeasible imidazolium-based IL. In this case, there is only one cation base (Eq. 12 is satisfied) and one anion (Eq. 13 is satisfied). The number of side chains are 2 which equates to the valence of cation (Eq. 14 is satisfied). The LHS of Constraint 4 (Eq. 15) translates to $(2 - 2)(1) + [(2 - 2)(1)(1) + (2 - 2)(1)(1)] + [(2 - 1)(1)(1) + (2 - 1)(1)(1)] = 2$, which equates to the RHS of the equation and hence Constraint 4, related to the whole cation, is satisfied. However, Constraint 5 (Eq. 16) related to the side chains are violated as follows: for side chain $l = 1$ containing two ethyl groups Eq. 16 translates to, $[(1)(1)(2 - 2) + (1)(1)(2 - 2)] \neq 1$, and for side chain $l = 3$ containing two methyl groups Eq. 16 translates to, $[(1)(1)(2 - 1) + (1)(1)(2 - 1)] \neq 1$. Therefore, the structure shown in Figure 4b is infeasible. For the structure shown in Figure 4c, Eqs. 12–14 are satisfied. The LHS of Constraint 4 (Eq. 15) translates to $(2 - 2)(1) + [(2 - 2)(1)(2) + (2 - 1)(1)(1)] + [(2 - 1)(1)(2)] = 3$, which does not equate to the RHS of the equation (i.e., 2) and hence Constraint 4, related to the whole cation, is violated. Constraint 5 (Eq. 16), related to the side chains translates to the following: for side chain position 1 (i.e., $l = 1$), LHS of Eq. 16 is $[(1)(2)(2 - 2) + (1)$

Table 1. Cation and Alkyl Side Chain Groups Valences

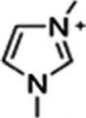
Cation Groups (c)	i	v_{ci}
	1	2
Alkyl Groups (k)	j	v_{Gkj}
CH ₃	1	1
CH ₂	1	2
CH ₃	3	1
CH ₂	3	2

Table 2. Values of y_l and ng_{kl} for 1,3-diethylimidazolium tetrafluoroborate

l	y_l	k	ng_{kl}
1	1	CH ₃	1
		CH ₂	1
3	1	CH ₃	1
		CH ₂	1

$(1)(2 - 1)] = 1$, which equates to the RHS of the equation (i.e., 1), but for side chain position 3 (i.e., $l = 3$) the same equation translates to $[(1)(2)(2 - 1)] = 2$ which does not equate to the RHS of the equation (i.e., 1) and hence Constraint 5, related to side chain 3, is violated. Therefore, the structure shown in Figure 4c violates two of the feasibility constraints and hence is infeasible.

Physical property constraints

IL structures play a key role in determining their unique physical properties. Physical property constraints utilize structure-property models which provide insights into the relationship between molecular structures and their properties. The particular type of structure-property relationships suited for CAILD are group contribution models (GC). As discussed before, GC models for physical properties are based on functional group additive principle. The IL is fragmented into characteristic groups and the property of interest is predicted as an additive function of the number of occurrence of a given group times its contribution to the pure component property. The contribution parameters of different groups are derived by correlating experimental data to a group additive expression. These models exist for several IL physical properties such as viscosity,²⁵ density,^{26–29} melting point,³⁰ electrical conductivity,³¹ thermal conductivity,³¹ heat capacities,³² solubility parameter,³³ and toxicity.³⁴

Solution property constraints

Thermodynamic properties of nonideal solutions are important for evaluating intermolecular interactions between multiple components (both ionic and molecular) present in a mixture. These thermodynamic properties are essential to evaluate the potential of ILs as solvents for reaction (solid solubility and liquid miscibility) and separation of fluid mixtures (liquid–liquid extraction and gas–liquid absorption). An essential requirement is the ability to predict excess Gibbs free energy (activity coefficients) of systems involving ILs which will enable prediction of equilibrium concentrations. These constraints are not only a function of binary/integer structure variables but also relate to the compositions of the various components of the mixture. The proposed CAILD framework requires models of activity coefficient that are based on solution of groups' concept. The basic hypothesis of the functional group concept is that interactions between molecules can be approximated as interactions between functional groups. The interaction amongst the groups of a mixture of an IL, [mIm][Tf₂N], and CH₃OH is shown in Figure 5.

The number of distinct cation head groups, anion groups, and alkyl groups are much less in comparison to the number of distinct ILs that can be generated from them. Therefore, a relatively small number of group interaction parameters are required to represent all possible ILs. UNIFAC³⁵ is a widely used GC model to predict phase equilibrium in nonelectrolyte systems. The UNIFAC method (UNiversal quasi-

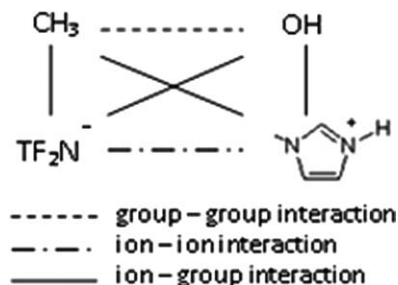


Figure 5. Different types of group interactions involved in solutions containing ionic species.

chemical Functional-group Activity Coefficients) uses the concept of functional groups to calculate activity coefficients. The activity coefficient has a combinatorial contribution (due to differences in size and shape of molecules) and residual contribution (due to energetic interactions).

$$\ln \gamma_i = \ln \gamma_i^C + \ln \gamma_i^R \quad (25)$$

The group volume (R) and surface area (Q) parameters of the combinatorial part are calculated as summation of group parameters (volume R_k and surface area Q_k) while binary group interaction parameters (a_{mn} and a_{nm}) are required for the calculation of the residual component. The UNIFAC approach was originally used for nonelectrolyte systems, however, in recent times several research groups have utilized this approach for ILs by careful representation of ionic groups and/or incorporating assumptions that factor the ionic nature of the groups. In order to apply the UNIFAC model, in its current form, to ILs Wang et al.³⁶ and Lei et al.³⁷ treated ionic groups as a single nondissociate neutral entity. For example, the IL $[\text{BmIm}]^+ [\text{BF}_4]^-$, was decomposed into two CH_3 groups, three CH_2 groups, and one $[\text{Im}][\text{BF}_4^-]$ group. Using the above representation Lei et al.³⁷ have added 12 new ionic groups (e.g., $[\text{Im}][\text{PF}_6]$) to the existing UNIFAC table. IL groups are being included in the modified UNIFAC (Dortmund) model.³⁸ Most recently, Roughton et al.³³ have characterized the ionic groups in the same way as proposed in our proposed CAILD formulation, that is, as separate cation base, anion, and alkyl groups. The underlying assumption here was that the ionic groups can be treated separately and the interactions between the ionic groups can be assumed to be zero due to the strong interaction and weak dissociation between ion pairs.³³ More detailed treatment of UNIFAC approach for ILs can be found in Roughton et al.,³³ Wang et al.,³⁶ and Lei et al.³⁷

Liquid–liquid equilibrium

Designing industrial scale liquid–liquid separation systems using IL requires modeling equilibrium relationships. In a non-ideal liquid mixture, species which have limited mutual solubility in the given liquid phase exhibit positive deviations from Raoult's law. The quantitative measure of nonideality is the liquid activity coefficient γ , which is a function of composition and temperature. If we identify the two liquid phases as l_1' and l_2' , their respective mole fractions in the two phases are related by the equilibrium condition as follows

$$\gamma^{l_1,i} x_{1,i} = \gamma^{l_2,i} x_{2,i} \quad (26)$$

where, $\gamma^{l_1,i}$ and $\gamma^{l_2,i}$ are activity coefficients of component i in the liquid phases 1 and 2, respectively, and $x_{1,i}$ and $x_{2,i}$ are mole fractions of component i in the two phases.

Solid–liquid equilibrium

Estimation of equilibrium saturation concentrations of solid–liquid systems is essential to model processes that involve solute dissolution and crystallization. The liquid phase activity coefficient predictions discussed before and pure component properties of solute (T_m , ...), can be utilized for these calculations.

$$\ln x_1^{\text{sat}} - \frac{\Delta_{\text{fus}} H}{T_m} \left(1 - \frac{T_m}{T} \right) + \ln \gamma_1^{\text{sat}} = 0 \quad (27)$$

where $\Delta_{\text{fus}} H$, T_m , and T represent enthalpy of fusion (J/mol), melting point (K) and temperature (K), respectively. γ_1^{sat} represents activity coefficient of solute at saturation and x_1^{sat} is the solubility of solute.

Solution of the underlying MINLP

The presented CAILD model is a nonconvex, MINLP problem, involving large number of integer and binary variables. Consideration of mixture properties through the UNIFAC model results in nonlinearity and most of the binary design variables (structural) participate in the nonlinear terms. Combinatorial complexity is an inherent issue in CAMD–MINLP models due to the nature of the search space. The most direct approach for solving the underlying MINLP model is complete enumeration. Generate and test methods fall under this category.²¹ Solution to the MINLP model can also be achieved through mathematical programming using deterministic (e.g. branch and bound,³⁹ branch and reduce⁴⁰) and stochastic optimization methods (e.g. simulated annealing,⁴¹ genetic algorithms (GAs),⁴² and Tabu search¹⁸). Approaches that combine features from both domains, such as decomposition methods, have also been previously developed.^{22,43} Achenie et al.¹⁴ provide a detailed description of various solution techniques in the context of molecular design problems. In this article, we focus on solving the CAILD framework utilizing two different methods: the decomposition methodology (includes generate and test algorithm) and GA-based optimization. The purpose is to demonstrate that different types of solution approaches can be used toward solution of the proposed CAILD formulation. Main details about the two approaches are provided below while in depth analysis can be found elsewhere.^{43,44}

Decomposition method

In this approach, the CAILD–MINLP model is decomposed into an ordered set of subproblems where each subproblem requires only the solution of a subset of constraints from the original set. As each subproblem is being solved large numbers of infeasible candidates are eliminated leading to a final smaller subproblem. The first subproblem usually consists of the structural constraints and it equates to enumeration. The second subproblem consists of pure component (physical) property constraints, whereas the third subproblem consists of mixture property constraints. These three subproblems taken together equate to generate and test methods. The IL candidates that pass through all of the above subproblems are the only ones that will be considered in the final optimization subproblem that involves the objective function, equilibrium relationships, and process models (if considered in the design problem). Most often, solution to the final subproblem can be achieved by solving a set of nonlinear programming problems.

Table 3. The Basis Set Used for Ionic Liquid Design.

Cations	Valency	Anions	Groups	Valency
Im	2	BF ₄ ⁻	CH ₃	1
mIm	1	PF ₆ ⁻	CH ₂	2
Py	2	Tf ₂ N ⁻		
mPy	1	Cl ⁻		

Genetic algorithm

GA is a method that can be used to solve optimization problems based on the natural selection process that mimics biological evolution. It can be applied to solve problems that are not well suited for standard optimization algorithms, including problems in which the objective function is discontinuous, nondifferentiable, stochastic, or highly nonlinear.⁴⁴ Unlike traditional search and optimization methods, GAs perform a guided stochastic search where improved solutions are achieved by sampling areas of the search space that have a higher probability for good solutions.⁴⁴ The optimization process starts with a collection of chromosomes (candidates). The fitter candidates are selected as “parents” and allowed to exchange or alter their genetic information, through crossover and mutation operations, with an aim to create more fitter off springs. At every iteration, new populations of offsprings are created to replace the existing population. This process of evolution is repeated for a predetermined number of generations or till the solution is found.⁴⁴ In GA, the selection of fitter parents for next generation is based on their fitness values as determined by a fitness function. The fitness function is usually very closely related to the original objective function of the search problem (in all of the case studies presented in this paper, the fitness function was identical to the objective function). The GA solution of CAILD model was implemented in the MATLAB environment with most parameters taking the default values. Specifically, for all the case study problems, the population size was fixed at 20 and the initial population was generated randomly. The crossover fraction was fixed at 0.8, whereas the mutation probability was fixed at 0.2. We allowed two candidates with the best fitness values (elite candidates) in the current generation to automatically survive to the next generation.

Case Studies

In this section, several case studies have been presented to illustrate the usefulness of the proposed approach. Table 3 lists the entire set of groups and their respective valences, from which the basis sets for the four case studies were derived. Note that this basis set covers only a small set of cations, anions, and functional groups for which GC parameters are currently available for the properties of interest. However, the design approach itself is universal in nature and upon availability of GC models and parameters can be easily extended (e.g., to all groups in Appendix A) to cover the entire spectrum of possible ILs. The maximum value allowed for the number of groups were fixed at 6 for each side chain and 12 for the whole cation.

Electrolytes

This case study demonstrates the design of an IL that has high electrical conductivity. Electrical conductivity measures the ability of a material to conduct electric current. It is an important property for the development of electrochemical

devices such as high energy batteries. Other requirements include the following: the electrolyte (i.e., IL) needs to be a room temperature ionic liquid (RTIL); and it should have reasonably low viscosity.

The electrical conductivity of ILs can be estimated using a Vogel-Tamman-Fulcher (VTF) type equation shown in Eq. 28

$$\ln \lambda = \ln A_{\lambda} + \frac{B_{\lambda}}{(T - T_{0\lambda})} \quad (28)$$

where A_{λ} , and B_{λ} , are adjustable parameters that can be obtained through GC expressions (Eqs. 29 and 30) as proposed by Gardas et al.,³¹ and $T_{0\lambda}$ has the value of 165 K for all considered IL types.

$$A_{\lambda} = \sum_{i=1}^k n_i a_{\lambda} \quad (29)$$

$$B_{\lambda} = \sum_{i=1}^k n_i b_{\lambda} \quad (30)$$

where n_i is the number of groups of type i and k is the total number of groups considered. Table 4 shows the GC parameters used.

The viscosity of ILs is calculated using an Orrick–Erbar-type approach.⁴⁵ In this method, viscosity (η , in cP) can be predicated as a function of density (ρ , in g cm⁻³) molecular weight (M), temperature (T), and parameters A and B through the use of Eq. 31.

$$\ln \frac{\eta}{\rho M} = A + \frac{B}{T} \quad (31)$$

We use the GC technique proposed by Gardas et al.³¹ to estimate the parameters A and B as follows

$$A = \sum_{i=1}^k n_i A_{v,i} \quad (32)$$

$$B = \sum_{i=1}^k n_i B_{v,i} \quad (33)$$

where n_i is the number of occurrences of group i (cation, anion, and functional groups) and $A_{v,i}$ and $B_{v,i}$ are the contributions of group i to the parameters A and B , respectively. The IL densities are estimated using the below formula.

$$\rho = \frac{M}{NV(a + bT + cP)} \quad (34)$$

where ρ the density in kg m⁻³, M is the molecular weight in kg mol⁻¹, N is the Avogadro number, V is the molar volume in Å³, T is the temperature in K, and P is the pressure

Table 4. Group Contributions for Parameters A_{λ} and B_{λ}

Species	a_{λ}	b_{λ} (K)
Im	77.8	-501.5
mIm	77.9	-537.6
Py	69.6	-544.9
mPy	69.7	-581.0
BF ₄ ⁻	85.8	-129.4
PF ₆ ⁻	117.3	-278.6
Tf ₂ N ⁻	10.1	-46.4
CH ₃	0.1	-36.1
CH ₂	0.1	-36.1

Table 5. Group Contributions for Parameters A, B and V

Species	ΔV	A_v	B_v
Im	84	8.04	1257.1
mIm	119	7.3	1507.1
Py	111	7.61	1453.6
mPy	146	6.87	1703.6
BF ₄ ⁻	73	-18.08	1192.4
PF ₆ ⁻	109	-20.49	2099.8
Tf ₂ N ⁻	248	-17.39	510.0
Cl ⁻	47	-27.63	5457.7
CH ₃	35	-0.74	250.0
CH ₂	28	-0.63	250.4

Table 6. σ_c Values for Different Cations

Type of Cation	σ_c Value
R = \dot{R} (Im, Pyr, Pip)	0.265
R \neq \dot{R} (Im, Pyr, Pip)	0.317
R or R and dimethylamino in C(4) (Py)	0.265

in MPa. Based on the data provided in Gardas et al.³¹, we developed GC parameters for molar volume with expressions similar to Eqs. 32 and 33. The values of coefficients a , b , and c are 0.8005 ± 0.0002 , $6.652 \times 10^{-4} \pm 0.007 \times 10^{-4} \text{ K}^{-1}$ and $-5.919 \times 10^{-4} \pm 0.024 \times 10^{-4} \text{ MPa}^{-1}$. Table 5 shows the GC parameters used in this model.

The melting point of ILs is estimated by a GC approach using Eq. 35 as proposed by Aguirre et al.⁴⁶

$$T_m = \frac{\sum_i n_i T_{m,i}}{a + \sigma_c + c\tau_c} \quad (35)$$

where n_i is the number of occurrences of group i (cation, anion, and functional groups) and $T_{m,i}$ is the contribution of group i to the melting point, a and c are constants with values of 0.1 and 0.012, respectively. τ_c , which is related to the cation flexibility, is estimated using Eq. 36 and σ_c is a cation symmetry parameter having values shown in Table 6.

$$\tau_c = \sum_k (n(\text{CH}_2)_k - 1) \quad (36)$$

The contribution, $T_{m,i}$, of different groups are listed in Table 7.

The CAILD design problem expressed in mathematical form is shown in Eq. 37–40.

Table 7. Group Contributions for Ionic Liquid Melting Point

Group	$T_{m,i}$
Im	107.99
mIm	109.88
Py	117.212
mPy	119.102
BF ₄ ⁻	-0.479
PF ₆ ⁻	16.746
Tf ₂ N ⁻	-0.966
Cl ⁻	35.852
CH ₃	-1.463
CH ₂	-1.463

Table 8. Decomposition Approach: Subproblem Results

Subproblem 1: Number of ionic liquids (ILs) generated, 138
Subproblem 2: Number of ILs satisfying pure component properties, 26
Subproblem 3: No mixture properties
Subproblem 4: Optimal IL, mIm [Tf ₂ N]

Objective Function.

$$f_{\text{obj}} = \max (\lambda) \quad (37)$$

Constraints.

$$\text{IL structural feasibility} \quad (38)$$

$$\eta < 65 \text{ cP} \quad (39)$$

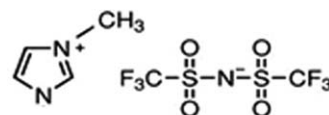
$$T_m < 298.15 \text{ K} \quad (40)$$

Results. *Decomposition approach.* The design statistics for this problem are summarized in Table 8. A total of 138 feasible IL structures were enumerated in Subproblem 1. Out of these, 26 ILs satisfied the physical property constraints (viscosity and melting point) in Subproblem 2. There were no mixture properties considered (Subproblem 3) and the solution to final subproblem (Subproblem 4) resulted in the optimal IL structure [1-methylimidazolium bis (trifluoromethylsulfonyl) imide] with the highest electrical conductivity (shown in Figure 6). The properties of the designed IL are listed in Table 9.

The same design problem (Eqs. 37–40) was solved using the GA toolkit in MATLAB (as explained in the Genetic algorithm section) and the program picked the exact same structure (shown in Figure 6) as the optimal solution.

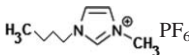
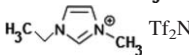
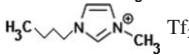
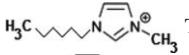
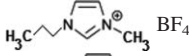
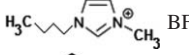
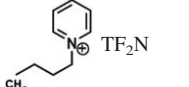
Analysis. In this section, we focus on the validation of design results through careful consideration and analysis of available experimental data. Table 10 lists the available experimental electrical conductivity, λ , (S/m) at 25°C for seven different ILs that are based on the cation, anion and side groups considered in this case study (Im, Py, PF₆, BF₄, Tf₂N, CH₃, and CH₂). Unfortunately, we could not find the electrical conductivity data for the designed IL [1-methylimidazolium bis (trifluoromethylsulfonyl) imide]. Therefore, we perform a qualitative IL structure-property trend analysis to validate the design results.

The electrical conductivity values have the following trend: $\lambda_{[\text{C}_4\text{mim}]\text{Tf}_2\text{N}} > \lambda_{[\text{C}_4\text{mim}]\text{BF}_4} > \lambda_{[\text{C}_4\text{mim}]\text{PF}_6}$. As, all of the above ILs have the same cation (C₄mim) but different

**Figure 6. 1-methylimidazolium [Tf₂N].****Table 9. Design Results of the Optimal IL 1-methylimidazolium [Tf₂N]**

Properties	Value
Melting point (K)	270.15
Viscosity (cP)	21.293
Electrical conductivity (S m ⁻¹) at 25°C	1.0956

Table 10. Experimentally Measured Electrical Conductivities of Ionic Liquids

Ionic liquid	T ($^{\circ}\text{C}$)	λ (S/m)	Ref.
	25	0.146	47
	25	0.912	47
	25	0.406	47
	25	0.218	47
	25	0.59	48
	25	0.35	48
	25	0.33	49

anions (TF_2N , PF_6 , and BF_4), we can infer that electrical conductivities of ILs with TF_2N anions are greater than those with PF_6 and BF_4 anions (for same cation and alkyl groups). The design result is consistent with this observation as the optimal structure has TF_2N anion. Similarly, by comparing the electrical conductivities of ILs having the same anion (TF_2N), we can see that $[\text{C}_2\text{mim}][\text{TF}_2\text{N}] > [\text{C}_4\text{mim}][\text{TF}_2\text{N}] > [\text{C}_6\text{mim}][\text{TF}_2\text{N}]$. Therefore, we can conclude that increasing the number of alkyl groups on the cation side chain decreases the electrical conductivity. The design result (Figure 6) is also consistent with this observation as there is only one methyl group (minimum needed to satisfy the cation valency) present in the cation side chain. Next, we compare the λ of $[\text{C}_4\text{mim}][\text{TF}_2\text{N}]$ and $[\text{C}_4\text{Py}][\text{TF}_2\text{N}]$ which have the same anion and different cations. We found experimental electrical conductivity data for $[\text{C}_4\text{Py}][\text{TF}_2\text{N}]$ but there was no data available for $[\text{C}_4\text{mPy}][\text{TF}_2\text{N}]$. As we already know that addition of alkyl groups to the cation base will decrease the electrical conductivity, we can infer that λ $[\text{C}_4\text{mPy}][\text{TF}_2\text{N}] < 0.33$ S/m (i.e., λ $[\text{C}_4\text{Py}][\text{TF}_2\text{N}]$) which in turn is much less than λ $[\text{C}_4\text{mim}][\text{TF}_2\text{N}]$ (0.406 S/m). Therefore, we can

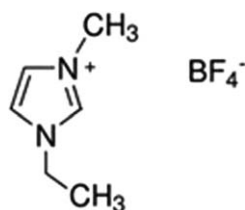


Figure 7. 1-ethyl-3-methylimidazolium $[\text{BF}_4]$.

Table 11. Group Contributions for Parameters A_k and B_k

Species	a_k	b_k (K^{-1})
Im	0.1272	0.000000104
mIm	0.1314	0.00000787
BF_4^-	0.0874	0.00008828
PF_6^-	0.0173	0.000009088
TF_2N^-	0.0039	0.00002325
Cl^-	0.0166	0.00001
CH_3	0.0042	0.000007768
CH_2	0.0010	0.000002586

Table 12. Decomposition Approach: Subproblem Results

Subproblem 1: Number of ionic liquids (ILs) generated, 92
Subproblem 2: Number of ILs satisfying pure component properties, 15
Subproblem 3: No mixture properties
Subproblem 4: Optimal IL, 1-ethyl-3-methylimidazolium tetrafluoroborate

conclude that electrical conductivity of ILs with imidazolium-based cations are greater than pyridinium-based cations (for same anion and alkyl groups). The design result is consistent with this observation as the optimal structure selected had an imidazolium cation. Overall, the model results are in full agreement with the observed trends from experiments, thereby validating the proposed approach.

Heat transfer fluids

ILs show great promise as heat transfer fluids and heat storage medium. High thermal conductivity is an important property for such applications. Thermal conductivity measures the ability of a material to conduct heat. Thermal conductivity of ILs is weakly dependent on temperature and could be fitted with the following linear correlation.

$$k = A_k - B_k T \quad (41)$$

where, k and T are the thermal conductivity in $\text{W m}^{-1} \text{K}^{-1}$ and temperature in K, respectively. We utilize a method²⁴ that uses GC approach to estimate the parameters A_k and B_k .

$$A_k = \sum_{i=1}^k n_i a_k \quad (42)$$

$$B_k = \sum_{i=1}^k n_i b_k \quad (43)$$

Table 11 shows the GC parameters that were used. Pyridinium and methyl pyridinium have not been considered in this part as their group contribution parameters were not found.³¹

Melting point and viscosity of ILs were calculated through the same methods proposed in case study 1. The CAILD design problem expressed as an optimization model is shown in Eqs. 44–47.

Objective Function.

$$f_{\text{obj}} = \max(k) \quad (44)$$

Constraints.

$$\text{IL structural feasibility} \quad (45)$$

$$\eta < 65 \text{ cP} \quad (46)$$

$$T_m < 298.15 \text{ K} \quad (47)$$

Results. Decomposition approach. The design statistics for this problem are summarized in Table 12. A total of 92 feasible IL structures were enumerated in Subproblem 1. Out of these, 15 ILs satisfied the physical property constraints (viscosity and melting point) in Subproblem 2. There were no mixture properties considered (Subproblem 3) and the solution to final subproblem (Subproblem 4) resulted in the optimal IL structure (1-ethyl-3-methylimidazolium tetrafluoroborate) with the highest thermal conductivity (shown in Figure 7). The properties of the designed IL are listed in Table 13.

The same design problem (Eqs. 44–47) was solved using the GA toolkit in MATLAB (as explained in the Genetic

Table 13. Design Results of the Optimal IL 1-ethyl-3-methylimidazolium [BF₄]

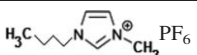
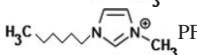
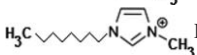
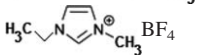

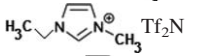
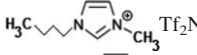
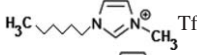
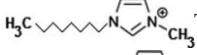
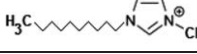
Properties	Value
Melting point (K)	291.71
Viscosity (cP)	60.75
Thermal conductivity (W m ⁻¹ K ⁻¹) at 25°C	0.193

algorithm section) and the program picked the exact same structure (shown in Figure 7) as the optimal solution.

Analysis

Table 14 shows experimental thermal conductivity, k [W m⁻¹ K⁻¹] for 10 different ILs that are based on the cation, anion, and side groups considered in this case study (Im, PF₆, BF₄, Tf₂N, CH₃, and CH₂). The designed IL (Figure 7) is same as the IL with the highest thermal conductivity value in Table 14 ([C₂mim] BF₄). This partially validates the results. However, for a more holistic assessment, we perform a qualitative IL structure-property trend analysis to determine whether the designed results are consistent with observed data. By comparing the thermal conductivity values (Table 14), we see that $k_{[C_4mim] BF_4} > k_{[C_4mim] PF_6} > k_{[C_4mim] Tf_2N}$. As all of these ILs have the same cation (C₄mim) but different anions (Tf₂N, PF₆ and BF₄), we can infer that thermal conductivities of ILs with BF₄ anions are greater than those with PF₆ and Tf₂N anions. The design result is consistent with this observation as the optimal structure has BF₄ anion. The only base cation considered in this design problem is imidazolium. By comparing the k values of different ILs with the same base cation and same anion, but different side groups, that is, [C₄mim] PF₆ vs. [C₆mim] PF₆ vs. [C₈mim] PF₆; and [C₂mim] Tf₂N vs. [C₄mim] Tf₂N vs. [C₆mim] Tf₂N vs. [C₈mim] Tf₂N vs. [C₁₀mim] Tf₂N, we can see that the contribution of alkyl side chain groups are not as high as that of anion, and there is no uniform trend that is observed in relation to varying number of alkyl side chain groups. Therefore, the optimal numbers of alkyl side chain groups relate to other requirements such as the IL needing to be a liquid (i.e., $T_m < 25^\circ\text{C}$ for RTILs) and have relatively low viscosity. Overall, we can conclude that the

Table 14. Experimental Thermal Conductivity Data

Ionic Liquid	T (K)	k (W m ⁻¹ K ⁻¹)	Ref.
 PF ₆	315	0.145	50
 PF ₆	315	0.146	50
 PF ₆	315	0.145	50
 BF ₄	315	0.1968	51
 BF ₄	315	0.1847	51
 Tf ₂ N	315	0.1294	52
 Tf ₂ N	315	0.1264	52
 Tf ₂ N	315	0.1263	52
 Tf ₂ N	315	0.12715	52
 Tf ₂ N	315	0.1299	52

design results are consistent with the observed experimental structure-property trends of thermal conductivity data.

Toluene–heptane separation

A common use of solvents in industrial processes is as a separating agent to separate two liquid components. This case study relates to the design of optimal IL to separate toluene (aromatic) and *n*-heptane (aliphatic). Sulfolane (C₄H₈O₂S) is a molecular solvent that is commonly used for this purpose. The design objective is to find an IL that can improve performance in comparison to sulfolane. One key requirement is to select an IL with as low viscosity as possible since, viscous solvents are not ideal from the stand point of industrial equipment design. The other requirement is to ensure that the designed solvent is a RTIL as the process requires a liquid solvent. A constraint on melting point (Eq. 56) is necessary to ensure design of RTILs only. Melting point and viscosity of ILs were calculated through the same methods proposed in Case Study 1. A good separation solvent should have a high value for selectivity (Eq. 48) and solvent power (Eq. 49), and low value for solvent loss (Eq. 50).

$$\text{Selectivity} : \beta = \frac{\gamma_{B,S}^\infty}{\gamma_{A,S}^\infty} \quad (48)$$

$$\text{Solvent power} : \text{SP} = \frac{1}{\gamma_{A,S}^\infty} \quad (49)$$

$$\text{Solvent loss} : \text{SL} = \frac{1}{\gamma_{S,B}^\infty} \quad (50)$$

The three properties are function of infinite dilution activity coefficients of the *n*-heptane/toluene/IL solution. The activity coefficients are calculated using the UNIFAC model and the interaction parameters for ILs were taken from Roughton et al.³³ Another important consideration is that, the addition of IL to the binary liquid mixture should result in the creation of two liquid phases. The appearance of new phases in a multicomponent system can be checked through the implementation of necessary and sufficient conditions for phase stability. These conditions for a ternary system, are shown in Eqs. 51 and 52. The activity coefficients were again calculated using the UNIFAC method as discussed before.

$$(1-x_2) \left(\frac{1}{x_2} + \frac{\partial \ln \gamma_2}{\partial x_2} \right) - x_3 \frac{\partial \ln \gamma_2}{\partial x_3} < 0 \quad (51)$$

$$\left(\frac{1}{x_2} + \frac{\partial \ln \gamma_2}{\partial x_2} \right) + \left(\frac{1}{x_3} + \frac{\partial \ln \gamma_3}{\partial x_3} \right) - \frac{\partial \ln \gamma_2}{\partial x_3} \cdot \frac{\partial \ln \gamma_3}{\partial x_2} < 0 \quad (52)$$

The CAILD design problem expressed as an optimization model is shown in Eqs. 53–58. It is worth mentioning that currently cost data is not available for ionic liquids as they are for the most part not commercially produced and it is also difficult to utilize cost information within a computer-aided molecular design framework. Hence cost was not considered for minimization.

Objective Function.

$$f_{\text{obj}} = \max (\beta) \quad (53)$$

Constraints.

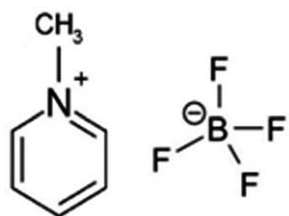
$$\text{IL structural feasibility (Eqs. 12–18)} \quad (54)$$

$$\eta < 65 \text{ cP} \quad (55)$$

$$T_m < 298.15 \text{ K} \quad (56)$$

Table 15. Decomposition Approach: Subproblem Results

Subproblem 1: Number of ionic liquids (ILs) generated, 185
 Subproblem 2: Number of ILs satisfying pure component properties, 27
 Subproblem 3: Number of ILs satisfying mixture properties, 1
 Subproblem 4: Optimal candidate, mPy [BF₄]

**Figure 8. 1-methylpyridinium [BF₄].**

$$SL < 0.0065 \quad (57)$$

$$SP > 0.3719 \quad (58)$$

Results. *Decomposition approach.* The design statistics for this problem are summarized in Table 15. A total of 185 feasible IL structures were enumerated in Subproblem 1 (structural constraints). Out of these, 27 ILs satisfied the physical property constraints (viscosity and melting point) in Subproblem 2. Out of these, one IL satisfied the mixture property constraints (Eqs. 57 and 58). The optimal IL structure (1-methylpyridinium tetrafluoroborate) with the highest selectivity is shown in Figure 8. The properties of the designed IL are listed in Table 16. Finally, we verified whether the designed IL created two phases when added to a hypothetical binary mixture consisting of 70% *n*-heptane (aliphatic) and 30% toluene (aromatic). This was accomplished by solving Eqs. 51 and 52 for a range of ternary compositions (keeping *n*-heptane to toluene ratio constant). We identified that phase split occurs at solvent composition range of 0.4–0.9.

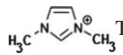
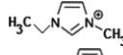
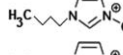
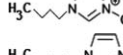
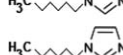
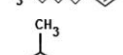
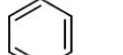
The structure of the optimal IL that satisfies all the constraints and has the maximum selectivity (β) is shown in Figure 8. The properties of the designed IL are listed in Table 16.

Analysis. Table 17 shows experimental selectivity values for separation of aromatics from an aromatic/aliphatic mixture using different ILs.⁵³ By comparing the selectivities for separation of benzene from benzene/heptane mixture, we see that $\beta_{[\text{hmim}]} \text{BF}_4 > \beta_{[\text{hmim}]} \text{PF}_6$. As both of these ILs have the same cation (hmim) but different anions (PF₆ and BF₄), we can infer that selectivities of IL with BF₄ anions are greater than those with PF₆ anions. By comparing the selectivities of [bmim] Tf₂N and [bmim] PF₆, (same cation and

Table 16. Design Results of the Optimal IL 1-methylpyridinium [BF₄]

Properties	1-methylpyridinium [BF ₄]	Sulfolane
Melting point (K)	294.8	300.65
Viscosity (cP)	55.084	10.07
SL	0.006471	0.0065 (<i>t</i> ₁)
SP	0.67193	0.3719 (<i>t</i> ₂)
β	87.262	6.8023 (<i>t</i> ₃)

Table 17. Experimentally Measured Selectivities for Aromatic/Aliphatic Separations

Solvent	Separation	<i>T</i> (°C)	β (selectivity)
 Tf ₂ N	Toluene/heptane	40	29.8
 Tf ₂ N	Toluene/heptane	40	22.2
 Tf ₂ N	Toluene/heptane	40	16.7
 PF ₆	Toluene/heptane	40	21.3
 PF ₆	Benzene/heptane	25	8.20
 BF ₄	Benzene/heptane	25	8.40
 BF ₄	Toluene/heptane	40	32.8

different anions), for separation of toluene/heptane mixture, we can infer that selectivities with PF₆ anion are greater than selectivities with Tf₂N anion. Therefore, we can conclude that among the anions used in the design problem (Tf₂N, PF₆, and BF₄), ionic liquids having BF₄ anion should have the highest selectivity toward aromatic compounds. The design result is consistent with this observation as the optimal IL has BF₄ anion. Similarly, by comparing the selectivities for separation of toluene/heptane mixture, we can see that $\beta_{[\text{mmim}]} \text{Tf}_2\text{N} > \beta_{[\text{emim}]} \text{Tf}_2\text{N} > \beta_{[\text{bmim}]} \text{Tf}_2\text{N}$. This shows that increasing number of alkyl groups on the cation side chain decreases the selectivity. The design result (Figure 8) is consistent with this observation also as there is only one methyl group (minimum needed to satisfy the cation valency) present in the cation side chain. With respect to cation, several studies have reported that pyridinium-based cations have higher selectivity than imidazolium-based cations for aliphatic/aromatic separation. This is also consistent with our design results as the optimal IL had pyridinium-based cation. This trend analysis qualitatively validates the CAILD methodology as well as the group interaction parameters (e.g., UNIFAC parameters provided in Roughon et al.) used in the model.

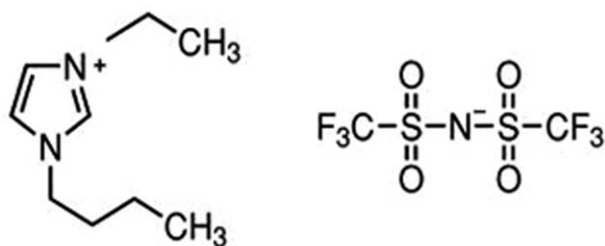
These qualitative trends from experiments are consistent with our CAILD results. The optimal design has a BF₄ anion and has minimal number of alkyl side groups (note that the selected methylpyridinium base cation needs at least one CH₃ group, that is, the minimum possible number of groups, to satisfy the valence requirement).

Naphthalene solubility

In this case study, we consider the design of an IL solvent for the dissolution of organic compound naphthalene. A molecular solvent having high solubility for naphthalene and commonly used for its dissolution is chloroform. The measured solubility of naphthalene in chloroform is 0.473 mole fraction.⁵⁴ Our objective is to find an IL that has higher solubility for naphthalene than chloroform. In addition, the IL needs to be an RTIL, and have a reasonably low viscosity. The melting point and viscosity are calculated using the

Table 18. Decomposition Approach: Subproblem Results

Subproblem 1: Number of ionic liquids (ILs) generated, 185
Subproblem 2: Number of ILs satisfying pure component properties, 27
Subproblem 3: Number of ILs satisfying mixture properties, 27
Subproblem 4: Optimal candidate, 1-butyl-3-ethylimidazolium [Tf ₂ N]

**Figure 9. 1-butyl-3-ethylimidazolium [Tf₂N].**

same models described in the Case Study 1. The expression shown in Eq. 61 is invoked to ensure solid–liquid phase equilibrium conditions, in order to determine the saturation concentration of solute (i.e., solubility).⁴³ The CAILD design problem expressed as an optimization model is shown in Eqs. 59–63.

Objective Function.

$$f_{\text{obj}} = \max(x_1^{\text{sat}}) \quad (59)$$

Constraints.

$$\text{IL structural feasibility} \quad (60)$$

$$\ln x_1 - \frac{\Delta_{\text{fus}} H}{T_m} \left(1 - \frac{T_m}{T}\right) + \ln \gamma_1^{\text{sat}} = 0 \quad (61)$$

$$\eta < 65 \text{ cP} \quad (62)$$

$$T_m < 298.15 \text{ K} \quad (63)$$

Results. Decomposition approach. The design statistics for this problem are summarized in Table 18. A total of 185 feasible IL structures were enumerated in Subproblem 1. Out of these, 27 ILs satisfied the physical property constraints (viscosity and melting point) in Subproblem 2. The optimal IL structure (1-butyl-3-ethylimidazolium [Tf₂N]) with the highest solubility is shown in Figure 9. The properties of the designed IL are listed in Table 19.

The structure of the optimal IL that satisfies the constraints is shown in Figure 9. The optimal properties of the designed IL are shown in Table 19.

Conclusions and Future Perspectives

An important component of green chemistry relates to the solvent medium in which synthetic transformations are carried out.⁵⁵ Traditional volatile organic solvents—which act as common reaction media for several chemical processes—are linked to a host of negative environmental and health effects including climate change, urban air-quality, and human illness. Jessop⁵⁶ states that one of the major challenges in the search for environmentally benign solvents is to ensure availability of green solvents as replacements for nongreen solvents of any kind. He uses the Kamlet–Taft plots to show that current list of green solvents populate only a small region of the entire spectrum of solvents needed

Table 19. Physical Properties of 1-butyl-3-ethylimidazolium [Tf₂N]

Properties	1-butyl-3-ethylimidazolium [Tf ₂ N]	Chloroform
Melting point (K)	222.78	209.65
Viscosity (cP)	55.59	0.542
Naphthalene solubility at 25°C	0.5069	0.473

for various applications and argues that large unpopulated areas of this diagram mean that future process chemists and engineers need solvents having certain desirable properties and are green. ILs offer great potential to satisfy this need.

This article presents an overarching framework that can be utilized to design optimal ILs for a given application through the theoretical/computational consideration of all possible combinations. Currently, the few IL structure-property models that are available can be applied to a small subset (e.g., the basis set shown in Table 3) of all available IL types. However, for this method to be fully effective, we need GC models and parameters that span the entire spectrum of ILs. It is indeed possible to overcome this challenge as one needs property values of only few representative compounds in each class of IL (e.g., covering the groups shown in Appendix A) to regress the contributions of the various groups. We propose that future research should focus on experimental property measurements and data collection of ILs that cover a diverse set of cations, anions, and functional groups. The second challenge is the lack of IL structure-property models (i.e., solution to the forward problem) for various thermo-physical properties of interest. There is a great need to develop structure-property models of pure-component physical properties and thermodynamic solution (mixture) properties for a comprehensive set of ionic groups. The third challenge would relate to the accuracy of the GC models. However, as discussed earlier, as the primary aim of the CAILD method would be to narrow down to a small set of ILs from the millions of available alternatives, reasonably accurate predictive models are sufficient. The final IL can be selected by *ab initio* computational chemistry calculation or experimental verifications of these small set of designed compounds.

Progress toward designing ILs through proposed CAILD, framework, will not only contribute toward our understanding of the relationship between cation–anion structures and IL properties, but will also provide a mechanism to engineer new environmentally benign ILs for critical applications.

Literature Cited

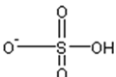
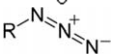

1. Rogers RD, Seddon KR. *Ionic Liquids as Green Solvents: Progress and Prospects*, 1st ed. Washington DC: American Chemical Society, 2003.
2. Walden P. Molecular weights and electrical conductivity of several fused salts. *Bull Acad Impér Sci (St Petersburg)*. 1914;405–422.
3. Armand M, Endres F, MacFarlane DR, Ohno H, Scrosati B. Ionic-liquid materials for the electrochemical challenges of the future. *Nat Mater*. 2009;8:621–629.
4. Zhang S, Sun N, He X, Lu X, Zhang X. Physical properties of ionic liquids: database and evaluation. *J Phys Chem Ref Data*. 2006;35:1475–1517.
5. Ionic Liquid Database-(IL Thermo). NIST standard reference database #147. Available at: <http://ilthermo.boulder.nist.gov/ILThermo/mainmenu.uix>. Last accessed data: 05/10/2013.
6. Holbrey JD, Seddon KR. Ionic liquids. *Clean Technol Environ Policy*. 1999;1:223–236.
7. Rogers RD, Seddon KR. Ionic liquids-solvents of the future? *Science*. 2003;302:792–793.

8. Ohno H. *Electrochemical Aspects of Ionic Liquids*. Hoboken: Wiley, 2005.
9. Wood N, Stephens G. Accelerating the discovery of biocompatible ionic liquids. *Phys Chem Chem Phys*. 2010;12:1670–1674.
10. Yan T, Burnham CJ, Delpopolo MG, Voth GA. Molecular dynamics simulation of ionic liquids: the effect of electronic polarizability. *J Phys Chem B*. 2004;108:11877–11881.
11. Cadena C, Magnin EJ. Molecular simulation study of some thermophysical and transport properties of triazolium-based ionic liquids. *J Phys Chem B*. 2006;110:18026–18039.
12. Kroon MC, Buijs W, Peters CJ, Witkamp GJ. Quantum chemical aided prediction of the thermal decomposition mechanisms and temperatures of ionic liquids. *Thermochem Acta*. 2007;465:40–47.
13. Vatamanu J, Borodin O, Smith GD. Molecular insights into the potential and temperature dependences of the differential capacitance of a room-temperature ionic liquid at graphite electrodes. *J Am Chem Soc*. 2010;132:14825–14833.
14. Achenie LEK, Gani R, Venkatasubramanian V. *Computer Aided Molecular Design: Theory and Practice*. Amsterdam: Elsevier Science, 2003.
15. Gani R, Brignole EA. Molecular design of solvents for liquid extraction based on UNIFAC. *Fluid Phase Equilib*. 1983;13:331–340.
16. Buxton A, Livingston AG, Pistikopoulos EN. Optimal design of solvent blends for environmental impact minimization. *AIChE J*. 1999;45:817–843.
17. Sinha M, Achenie LEK, Gani R. Blanket wash solvent blend design using interval analysis. *Ind Eng Chem Res*. 2003;42:516–527.
18. Chavali S, Lin B, Miller DC, Camarda KV. Environmentally-benign transition metal catalyst design using optimization techniques. *Comput Chem Eng*. 2004;28:605–611.
19. Karunanithi AT, Achenie LEK, Gani R. A computer-aided molecular design framework for crystallization solvent design. *Chem Eng Sci*. 2006;61:1247–1260.
20. Chemmangattuvalappil NG, Eljack FT, Solvason CC, Eden MR. A novel algorithm for molecular synthesis using enhanced property operators. *Comput Chem Eng*. 2009;33:636–643.
21. Harper PM, Gani R, Kolar P, Ishikawa T. Computer-aided molecular design with combined molecular modeling and group contribution. *Fluid Phase Equilib*. 1999;158–160:337–347.
22. Samudra AP, Sahinidis NV. Optimization-based framework for computer-aided molecular design. *AIChE J*. 2013;59:3686–3701.
23. Sheldon TJ, Folic M, Adjiman CS. Solvent design using a quantum mechanical continuum solvation model. *Ind Eng Chem Res*. 2006;45:1128–1140.
24. Odele O, Machietto S. Computer aided molecular design: a novel method for optimal solvent selection. *Fluid Phase Equilib*. 1993;82:47–54.
25. Gardas RL, Coutinho JAP. A group contribution method for viscosity estimation of ionic liquids. *Fluid Phase Equilib*. 2008;266:195–201.
26. Valderrama JO, Reategui A, Rojas RE. Density of ionic liquids using group contribution and artificial neural networks. *Ind Eng Chem Res*. 2009;48:3254–3259.
27. Qiao Y, Ma Y, Huo Y, Ma P, Xia S. A group contribution method to estimate the densities of ionic liquids. *J Chem Thermodyn*. 2010;42:852–855.
28. Ye C, Shreeve JM. Rapid and accurate estimation of densities of room-temperature ionic liquids and salts. *J Phys Chem A*. 2007;111:1456–1461.
29. Gardas RL, Coutinho JAP. Extension of the Ye and Shreeve group contribution method for density estimation of ionic liquids in a wide range of temperatures and pressures. *Fluid Phase Equilib*. 2008;263:26–32.
30. Huo Y, Xia S, Zhang Y, Ma P. Group contribution method for predicting melting points of imidazolium and benzimidazolium ionic liquids. *Ind Eng Chem Res*. 2009;48:2212–2217.
31. Gardas RL, Coutinho JAP. Group contribution methods for the prediction of thermophysical and transport properties of ionic liquids. *AIChE J*. 2009;55:1274–1290.
32. Gardas RL, Coutinho JAP. A group contribution method for heat capacity estimation of ionic liquids. *Ind Eng Chem Res*. 2008;47:5751–5757.
33. Roughton BC, Christian B, White J, Camarda KV, Gani R. Simultaneous design of ionic liquid entrainers and energy efficient azeotropic separation processes. *Comput Chem Eng*. 2012;42:248–262.
34. Luis P, Ortiz I, Aldaco R, Irabien A. A novel group contribution method in the development of a QSAR for predicting the toxicity (*Vibrio fischeri* EC50) of ionic liquids. *Ecotoxicol Environ Saf*. 2007;67:423–429.
35. Fredenslund A, Jones RL, Prausnitz JM. Group-contribution estimation of activity coefficients in nonideal liquid mixtures. *AIChE J*. 1975;21:1086–1099.
36. Wang J, Sun W, Li C, Wang Z. Correlation of infinite dilution activity coefficient of solute in ionic liquid using UNIFAC model. *Fluid Phase Equilib*. 2008;264:235–241.
37. Lei Z, Zhang J, Li Q, Chen B. UNIFAC model for ionic liquids. *Ind Eng Chem Res*. 2009;48:2697–2704.
38. Nebig S, Gmehling J. Prediction of phase equilibria and excess properties for systems with ionic liquids using modified UNIFAC: typical results and present status of the modified UNIFAC matrix for ionic liquids. *Fluid Phase Equilib*. 2011;302:220–225.
39. Sinha M, Achenie LEK, Ostrovsky GM. Environmentally benign solvent design by global optimization. *Comput Chem Eng*. 1999;23:1381–1394.
40. Sahinidis NV, Tawarmalani M. Applications of global optimization to process and molecular design. *Comput Chem Eng*. 2000;24:2157–2169.
41. Marcoulaki EC, Kokossis AC. On the development of novel chemicals using a systematic synthesis approach. *Part I. Optimisation framework*. *Chem Eng Sci*. 2000;55:2529–2546.
42. Xu W, Diwekar UM. Improved genetic algorithms for deterministic optimization and optimization under uncertainty. *Part II. Solvent selection under uncertainty*. *Ind Eng Chem Res*. 2005;44:7138–7146.
43. Karunanithi AT, Achenie LEK, Gani R. A new decomposition-based computer-aided molecular/mixture design methodology for the design of optimal solvents and solvent mixtures. *Ind Eng Chem Res*. 2005;44:4785–4797.
44. Patkar PR, Venkatasubramanian V. Genetic Algorithms Based CAMD. In: Achenie LEK, Gani R, Venkatasubramanian V, editor. *Computer Aided Molecular Design: Theory and Practice*. Amsterdam: Elsevier Science, 2003.
45. Reid RC, Prausnitz JM, Sherwood TK. *The Properties of Gases and Liquids*, 4th ed. New York: McGraw-Hill, 1987.
46. Aguirre CL, Cisternas LA, Valderrama JO. Melting-point estimation of ionic liquids by a group contribution method. *Int J Thermophys*. 2012;33:34–46.
47. Widegren JA, Saurer EM, Marsh KN, Magee JW. Electrolytic conductivity of four imidazolium-based room-temperature ionic liquids and the effect of a water impurity. *J Chem Thermodyn*. 2005;37:569–575.
48. Nishida T, Tashiro Y, Yamamoto M. Physical and electrochemical properties of 1-alkyl-3-methylimidazolium tetrafluoroborate for electrolyte. *J Fluor Chem*. 2003;120:135–141.
49. Tokuda H, Tsuzuki S, Susan ABH, Hayamizu K, Watanabe M. How ionic are room-temperature ionic liquids? an indicator of the physicochemical properties. *J Phys Chem B*. 2006;110:19593–19600.
50. Tomida D, Kenmochi S, Tsukada T, Qiao K, Yokoyama C. Thermal conductivities of [bmim][PF₆], [hmim][PF₆], and [omim][PF₆] from 294 to 335 K at pressures up to 20 MPa. *Int J Thermophys*. 2007;28:1147–1160.
51. Valkenburg MEV, Vaughn RL, Williams M, Wilkes JS. Thermochemistry of ionic liquid heat-transfer fluids. *Thermochim Acta*. 2005;425:181–188.
52. Ge R, Hardacre C, Nancarrow P, Rooney DW. Thermal conductivities of ionic liquids over the temperature range from 293 K to 353 K. *J Chem Eng Data*. 2007;52:1819–1823.
53. Meindersma GW, Podt A (JG), Haan AB. Selection of ionic liquids for the extraction of aromatic hydrocarbons from aromatic/aliphatic mixtures. *Fuel Process Technol*. 2005;87:59–70.
54. Gmehling JG, Anderson TF, Prausnitz JM. Solid-liquid equilibria using UNIFAC. *Ind Eng Chem Fundam*. 1978;17:269–273.
55. Anastas PT, Warner JC. *Green Chemistry: Theory and Practice*. Oxford: Oxford University Press, 2000.
56. Jessop PG. Searching for green solvents. *Green Chem*. 2011;13:1391–1398.

Appendix A

Cation	Structure	Valency	Anion	Structure	Groups	Valency
Imidazolium		1				
		2	BF_4^-		CH_3	1
		3				
		4				
		5				
Pyridinium		Possible values 1,2,3,4,5,6	PF_6^-		CH_2	2
Pyrrolidinium		Possible values 1,2,3,4,5,6	Tf_2N^-		CH	3
Ammonium		Possible values 1,2,3,4	Halogen	Cl^- , Br^- ,	$\text{C}=\text{}$	2
Phosphonium		Possible values 1,2,3,4	Mesylate		$\text{C}\equiv$	1
Piperidinium		Possible values 1,2,3,4,5,6,7	Propionate		OH	1
Triazolium		Possible values 1,2,3,4,5	Benzoate		ACH	2
Thiazolium		Possible values 1,2,3,4	Acetate		AC	3
Pyrazinium		Possible values 1,2,3,4,5	Trifluoroacetate		$\text{CH}_3\text{C}=\text{O}$	1
Sulfonium		Possible values 1,2,3	Phosphate		$\text{CH}_2\text{C}=\text{O}$	2
			Toluenesulfonate		HCO	1

Appendix A Table Continued

Cation	Structure	Valency	Anion	Structure	Groups	Valency
			Hydrosulfate		CH ₃ COO	1
			Azide		CH ₂ COO	2
			Perchlorate		HCOO	1
					CH ₃ O	1
					CH ₂ O	2
					CHO	3
					CH ₂ NH ₂	1
					CHNH ₂	2
					COOH	1
					COO	1
					CH ₃ S	1
					CH ₂ S	2

Manuscript received Dec. 6, 2012; revision received May 12, 2013; and final revision received Aug. 30, 2013.